Energy analysis of two stage packed-bed chemical looping combustion configurations for integrated gasification combined cycles

H.P. Hamers [a], M.C. Romano [b,*], V. Spallina [a], P. Chiesa [b], F. Gallucci [a], M. van Sint Annaland [a]

[a] Chemical Process Intensification, Department of Chemical Engineering and Chemistry, Eindhoven University of Technology, P.O. Box 513, 5600MB Eindhoven, The Netherlands
[b] Group of Energy Conversion Systems, Department of Energy, Politecnico di Milano, Via Lambruschini 4, 20156 Milano, Italy

Received 11 October 2014 Received in revised form
4 March 2015
Accepted 25 March 2015 Available online 1 May 2015

1. Introduction

Due to increasing concerns about climate change, CCS (carbon capture and storage) is regarded as an interesting mid-term solution to mitigate anthropogenic CO_2 emissions. If CCS is applied to a power production process, an additional energy penalty results mainly related to the separation of the produced CO_2 from the flue gas stream. CLC (chemical-looping combustion) is a technology in which the separation of the CO_2 is integrated with the power production process by avoiding direct contact between the fuel and air and thereby dilution of the CO_2 rich exhaust stream with N_2. The fuel is combusted with an oxygen carrier (supported metal oxide particle) producing a CO_2/H_2O mixture while the oxygen carrier is reduced. The oxygen carrier is subsequently oxidized to its original state with air. The sum of these reactions (listed for syngas as fuel in Equation (1)) is equal to a regular combustion reaction. So, the total reaction enthalpy is the same as with regular fuel combustion. Such a system, thanks to the intrinsic separation of the CO_2 reaction product, leads to a higher electrical efficiency of the complete plant with respect to most of the other carbon capture technologies [1,2].

$$\begin{aligned} &n\,H_2 + n\,MeO \rightarrow n\,H_2O + n\,Me \\ &m\,CO + m\,MeO \rightarrow m\,CO_2 + m\,Me \\ &\frac{n+m}{2}O_2 + (n+m)Me \rightarrow (n+m)MeO \\ &\hline n\,H_2 + m\,CO + \tfrac{n+m}{2}O_2 \rightarrow n\,H_2O + m\,CO_2 \end{aligned} \quad (1)$$

In general, CLC can be applied to power plants fueled with natural gas, coals or biomass. Solids can be fed directly to the CLC reactors, leading to a relatively simple and high-efficiency power plant configuration. However, problems regarding full conversion of the fuel to CO_2 and H_2O have been observed in experimental

* Corresponding author. Tel.: +39 02 2399 3846; fax: +39 02 2399 3913.
E-mail address: matteo.romano@polimi.it (M.C. Romano).

Abbreviations

AGR	acid gas removal
ASU	air separation unit
CCS	carbon capture and storage
CLC	chemical looping combustion
HHV	high heating value
HP	high pressure
HRSG	heat recovery steam generator
IGCC	integrated gasification combined cycle
IP	intermediate pressure
LHV	low heating value
LP	low pressure
SPECCA	specific primary energy consumptions for CO_2 Avoided, MJ_{LHV}/kg_{CO2}
TSA	temperature swing adsorption
TS-CLC	two stage chemical-looping combustion

Symbols

b	stoichiometric factor in the redox reactions, mol solid/mol gas
C	concentration, mol m^{-3}
C_p	heat capacity, J mol^{-1} K^{-1}
D	reactor inner diameter, m
D_a	diameter at the interface of the internal refractory and the steel vessel, m
D_{ax}	axial dispersion coefficient, m^2 s^{-1}
d_p	particle diameter, m
E_A	activation energy, J mol^{-1}
f	design stress of carbon steel, Pa
ΔH_R	enthalpy of reaction, J mol^{-1}
k_0	pre-exponential factor, $mol^{1-n}m^{3n-3}s^{-1}$
L	reactor length, m
M	molar mass, kg/mol
$\dot{M}$	molar flow rate, kmol/s
$\dot{m}$	mass flow rate, kg/s
$\dot{m}_s$	specific mass flow rate, kg/(m^2s)
n	reaction order in gas, -
N_R	number of reactors, -
Nu	Nusselt number, -
p	pressure, Pa
Pr	Prandtl number, -
R	gas constant, J mol^{-1} K^{-1}
r	reaction rate, mol m^{-3} s^{-1}
Re	Reynolds number, -
Sc	Schmidt number, -
T	temperature, K
$T_{max,CLC}$	temperature inside reactor, K
T_{steel}	temperature of the steel vessel, K
t	time, s
V_R	volume of reactor, m^3
v	superficial velocity, m s^{-1}
x	axial position, m
X	particle conversion, -
y	mole fraction in gas feed, -
red	reduction
p1	purge1
ox	oxidation
HR	heat removal
p2	purge2

Greek letters

ε	porosity, m^3 m^{-3}
ζ	stoichiometric factor, mol gas/mol solid
λ_{eff}	effective heat dispersion coefficient, W m^{-1} K^{-1}
λ_r	heat conductivity of refractory, W m^{-1} K^{-1}
η_g	dynamic gas viscosity, kg m^{-1} s^{-1}
ρ	density, kg/m^3
$\rho_{mol,oxygen}$	amount of atomic oxygen per m^3 of reactor, kmol/m^3
τ	cycle time, s
ω	mass fraction, kg kg^{-1}

subscripts

act	active
avg	average
i	gas component
in	inlet
j	solid component
p	particle
r	refractory
red	reduction
eff	effective
g	gas
s	solid

superscripts

in	inlet
0	initial

tests [3], which indicate that further process developments are required or a complete novel fuel reactor design [4]. Also, the separation of the uncombusted char from the oxygen carrier transported from the fuel to the air reactor and the recovery of the oxygen carrier from the ash purged from the system have to be performed in dedicated vessels. As an alternative option to the direct utilization, solid fuels can be first gasified in a gasifier into a CO/H_2-based syngas, which is first purified and afterwards fed to the CLC reactor(s). In this work, the latter option of the IGCLC (integrated gasification CLC) plant is considered. The electrical efficiency for IGCLC plants has been calculated by several researchers, based either on fluidized bed [1,5–7] or packed bed [2] CLC processes. Erlach et al. [1] and Spallina et al. [2] also compared the performance of IGCLC plants using nickel and ilmenite respectively as oxygen carriers with benchmark plants, demonstrating that in an IGCLC power plant a higher electrical efficiency can be obtained than with conventional pre-combustion CO_2 capture. Improvements by 3–5 percentage points have been reported in these works [1,2]. The packed bed and the circulating fluidized bed configurations for CLC have been compared as well resulting in minor differences regarding the overall process efficiency [8].

The highest electrical efficiency can be achieved by a combined cycle that consists of a gas turbine and a heat recovery steam cycle. To apply this configuration efficiently, the gas for the gas turbine has to be produced with CLC at around 1200 °C and 20 bar [9,10]. At these operating conditions it is very challenging to obtain stable solid circulation and to completely separate the gases and solids by cyclones in a circulated fluidized bed system (especially because of the fines produced in such reactor systems). To circumvent these limitations, dynamically operated packed beds have been proposed where the solids are stationary and the gas streams are switched periodically [11,12]. With packed bed technology, problems with

fines production and gas solid separation are intrinsically circumvented.

A packed bed CLC reactor is a batch reactor that undergoes the following steps: reduction, oxidation, heat removal and purge. First, the carrier (MeO) is reduced with syngas, then the reactor is purged with N_2 to prevent contact between air and syngas. Subsequently, the carrier is oxidized with air causing a temperature rise inside the reactor (highly exothermic reaction). Afterwards, the heat is removed during the heat removal step and the cycle is finished by a purge with N_2. By operating with several reactors in parallel with at least one in each different phase, a continuous in- and out-flow of gas can be kept in each reactor and through all the other plant components (turbomachines, heat exchangers, etc …).

If air is pressurized from ambient conditions up to 20 bar, a temperature of about 450 °C is obtained. If a turbine inlet temperature of 1200 °C has to be reached, a large temperature rise of about 750 °C has to be achieved inside the packed bed reactor. This puts a high demand on the oxygen carrier selection (thermal and chemical stability) and the reactor material. Considering the most studied oxygen carriers, only nickel oxide and ilmenite could be applied to achieve such ΔT, but both have some important drawbacks. Nickel is an expensive and toxic material [13], while ilmenite has a low reactivity at low temperatures [14]. The low reactivity of ilmenite can be circumvented by carrying out the reduction just after the oxidation when the bed is at high temperature and then performing the heat removal on the reduced bed by means of a N_2 stream [14]. Spallina et al. showed that a high efficiency can be obtained in this case by means of a semi-closed N_2-based gas turbine cycle for power generation [2].

A large number of the papers published about CLC focuses on the selection of a suitable oxygen carrier, which might be the most difficult challenge in this research field [3]. To reduce the demands on the oxygen carriers and achieve the same overall ΔT, the novel Two Stage Chemical Looping Combustion (TS-CLC) configuration has been proposed in a previous work [13], where the heat is produced via two packed beds placed in series. A schematic overview of this configuration is shown in Fig. 1. Initially, both reactors have a different temperature: the first bed is at 450 °C (i.e. the compressed air temperature) and the second is at around 850 °C. In step 1, the bed is reduced with syngas, resulting in a small temperature rise in both reactors. After a purge with N_2, the bed is oxidized with air and temperatures of 850 °C and 1200 °C are reached in the first bed and in the second bed respectively. In the third step, the heat removal, the heat from the first bed is blown to the second bed, while a gas stream at 1200 °C is formed in the second reactor that is fed to the gas turbine. Subsequently, the reactors are purged and the same temperature profile is obtained as at the beginning of the cycle. In the first reactor, for example a copper-based oxygen carrier can be used, because it has a high reactivity at low temperatures. The main disadvantage of copper is its low melting point, but this is not an issue in this concept, because the maximum temperature in the first reactor is lower than the melting point of copper. In the second reactor, a manganese-based oxygen carrier can be used, because of its good stability at high temperatures. The problem of utilizing manganese as oxygen carrier in a single stage CLC process is that a high active weight content is needed for a temperature increase of 750 °C (51wt%) and it is difficult (if not impossible) to develop an oxygen carrier with such a high active weight content with a high mechanical (and thermal) stability. Conversely, in the two stage configuration, the desired temperature rise for the second reactor is smaller and therefore a smaller active weight content suffices.

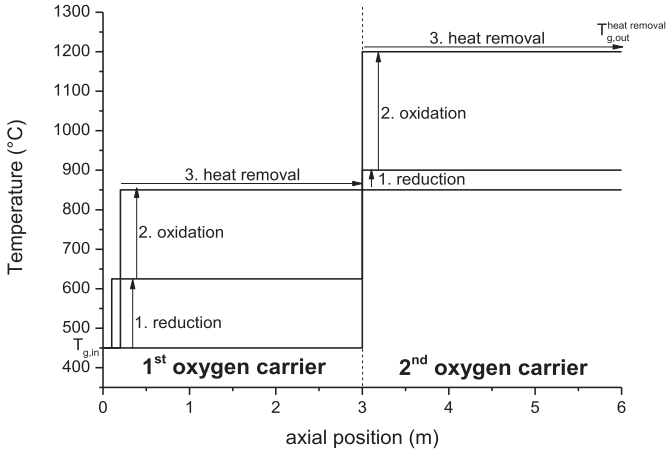

Fig. 1. Schematic overview of the TS-CLC configuration and axial temperature profiles assuming infinite redox kinetics and absence of heat dispersion in the axial direction [13].

1D reactor model results have demonstrated that it could indeed be a feasible solution to produce air at 1200 °C, but much more heat dispersion is observed inside the reactor compared to the idealized profiles shown in Fig. 1. Hence, CO_2 and H_2O are produced at higher temperature and a slightly lower quantity of hot air is produced for the gas turbine [13]. This could affect the overall electrical efficiency and a more detailed energy analysis of the complete system is required to assess the energy efficiency of this system, which is the focus of the present paper.

In this work, the newly developed TS-CLC configuration using copper and manganese based oxygen carriers is compared with a one stage nickel-based packed bed CLC, integrated in a complete IGCLC plant, through process simulations. The aim is to compare the novel TS-CLC system with the classical CLC system already assessed in the literature, on the basis of the electrical efficiency. An estimation of the investment costs for the CLC reactors is made to ensure that the flexibility in terms of oxygen carrier selection of the TS-CLC is not paid by higher investment costs.

In the next section, first the power plant configuration and modeling assumptions are described. Subsequently, the CLC reactor design for both cases is discussed and compared, and a preliminary estimation is made of the initial investment costs for both configurations. Afterwards, the process efficiencies of the different packed bed CLC configurations are evaluated.

2. Method and assumptions

For the case of the one stage CLC, a 19 wt% NiO/Al_2O_3 was selected as oxygen carrier, because this is currently the only feasible oxygen carrier in a packed bed, if the reduction is carried out at low temperature [13]. In the TS-CLC cases, the first reactor contains CuO/Al_2O_3 and the second reactor Mn_3O_4/Al_2O_3.

2.1. IGCLC power plant description

The IGCLC power plant has been simulated with the GS software developed at the Department of Energy of Politecnico di Milano [15]. It is a software in which complex power plants are reproduced by assembling basic modules. The main feature of the code is the use of built-in correlations to estimate the efficiency of the turbomachines. In particular, steam and gas turbines are calculated based on a stage-by-stage approach [16,17]. Gas turbine calculation includes routines to estimate the cooling flows needed in each stage and their effect on the stage efficiency. The thermodynamic properties of gases are based on NASA (National Aeronautics and Space Administration) polynomials [18] regressed on JANAF (Joint Army, Navy, Air Force) tables data [19], while the water/steam properties

are taken from steam tables [20]. The temperature of the produced streams in the CLC process depends on how the heat fronts develop through the CLC reactors during operation. To achieve an accurate evaluation of this temperature, a 1D model was used to simulate the packed bed reactors for CLC [12]. The packed bed reactors have been sized and the number of reactors is calculated based on the selected total cycle time (total time for all the operation steps) and pressure drop.

A simplified scheme of the IGCLC power plant is shown in Fig. 2. A detailed power plant scheme, extended description, detailed mass balance and an overview of the assumptions can be found in Spallina et al. [2]. In this work, a global description is given of the gasification section, while the CLC section is discussed in more detail.

The composition of coal is based on bituminous South African Douglas Premium Coal with 8wt% moisture content, which was published as reference for power plant calculations in [21]. First, the coal is pulverized and dried to a moisture content of 2 wt%. Then the coal is pressurized to 44 bar by CO_2 in the lock hoppers and this is fed to a Shell gasifier. The oxidant for the gasification is supplied by steam and oxygen from the ASU (air separation unit). After the gasifier, the outlet stream is cooled down and high and intermediate pressure steam is produced. Subsequently, the syngas is treated and desulfurized by Selexol process. Afterwards, the pressure is reduced to 21.6 bar and the syngas is fed to the saturator to increase the humidity and the temperature. The syngas leaves the saturator at 151 °C and it is heated up to 300 °C by saturated water withdrawn from the high pressure drum. Then 33.4 kg/s steam (stream #17) is mixed to avoid carbon deposition inside the CLC reactor. The amount of steam is adjusted so that no carbon deposition can thermodynamically occur at 20 bar above 450 °C. The dilution with steam is useful to avoid both coke deposition in the CLC bed and metal dusting in the high temperature fuel heater.

Before the syngas is fed to the CLC reactor, it is further heated up to 600 °C in a gas–gas heat exchanger with the CO_2/H_2O stream from the CLC unit. The syngas is extra preheated, because better temperature profiles are obtained in the packed bed reactors. The syngas (#1) is fed to the CLC reduction reactors with the following composition: 32.1% CO, 5.3% CO_2, 13.1% H_2, 48.3% H_2O, 0.7% N_2 and 0.6% Ar. In the CLC reactors, a mixture of CO_2 and H_2O (#2) is produced at a temperature dependent on the configuration of the CLC system. During the cooling of this stream, heat is recovered by generating superheated steam at 565 °C (#13). The temperature of the CO_2/H_2O is fluctuating (in time) and therefore measures to avoid too large temperature fluctuations of the hot heat exchanger surface are needed to avoid excessive thermal fatigue of the tubes material. For example, proper arrangement of the heat transfer banks, controlled mixing with recycled cooler CO_2 or buffering with inert material in a fixed or fluidized bed vessel could be considered to reduce the stress for the heat exchangers. Afterwards, heat is recovered by high pressure water which is heated up to the saturation temperature. Some low pressure steam is formed as well and some low temperature heat is used to increase the temperature of part of the water from the condenser. Afterwards, the CO_2/H_2O stream exiting the heat recovery section (#3) is further cooled to 35 °C with cooling water, condensate is separated and the CO_2 is compressed by an intercooled compression process and pumped to 110 bar (#4). The electricity consumption for the CO_2 compression has been calculated in Aspen Plus [22].

The oxygen carrier is oxidized by atmospheric air (#5, at 15 °C), pressurized to 20 bar and 438 °C (#6). This air is used for the oxidation reaction, the heat removal and for cooling the blades of the first two gas turbine stages. After the oxidation reaction, N_2 is obtained at 575 °C. This N_2 is reused by mixing it with the air that is going to the CLC reactor for the heat removal step. In this way, the heat of the N_2 is reused in the system. As a result, the temperature of the heat removal stream is slightly higher (#8, about 466 °C) and therefore the subsequent reduction can be carried out at a slightly higher temperature. The reduction temperature is one of the most critical parameters for the oxygen carrier selection, so a higher temperature could be quite beneficial as it increases the reduction

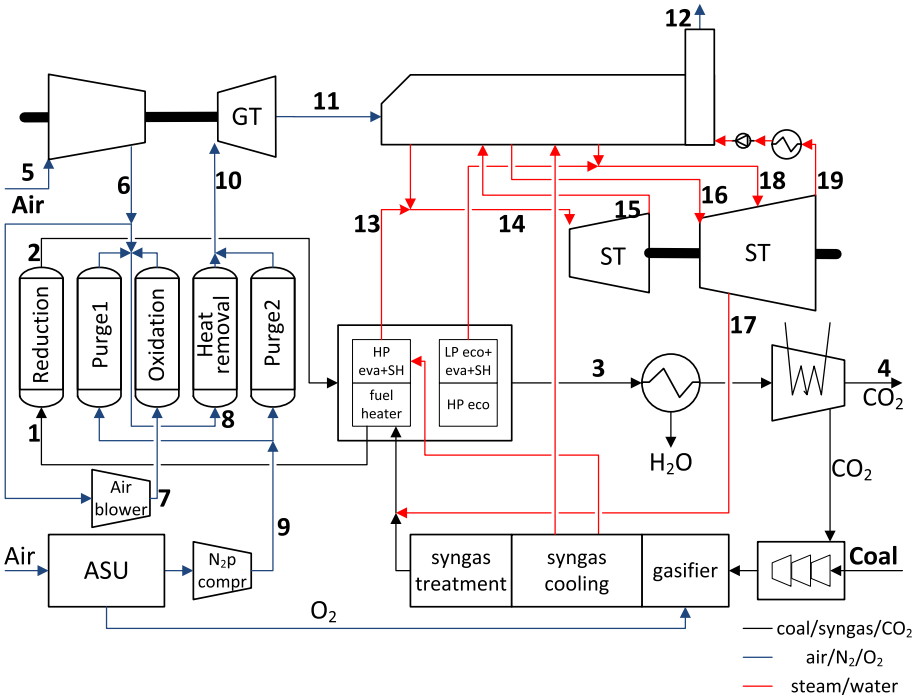

Fig. 2. The simplified IGCLC power plant scheme. The main properties (temperature, pressure and flow rate) of the streams shown in the figure are reported further on in Table 9 for the three assessed plants.

kinetics. The outlet from the oxidation should be at 20 bar (as the air with which it is mixed) and therefore the air for oxidation (#7) is compressed by an additional compressor to a pressure slightly higher than 20 bar (to overcome the pressure drop in the reactors).

Between oxidation and reduction steps, the reactor needs to be purged with N_2 from the ASU.[1] This stream is pressurized and fed to the packed bed reactors at 478 °C and 20.4 bar (#9). The purge outlet is mixed with the heat removal stream.

The heat removal stream is fed to the gas turbine at 1200 °C and 19 bar (#10). In the gas turbine, the gas is expanded and sent to the heat recovery steam generator (#11), where steam is generated at three different pressure levels, 144 bar, 36 bar and 4 bar. The cooled O_2 depleted air is finally vented by a stack (#12). Steam turbine is fed with high pressure steam (#14), with intermediate pressure steam (#16) obtained from the reheating of the steam from the HP turbine (#15) and low pressure steam (#18). The steam discharged from the turbine (#19) is then condensed and returned to the HRSG (heat recovery steam generator).

2.2. Packed bed reactor model for CLC reactors

The packed bed reactors are described in more detail by a 1D packed bed reactor model. In this model, the mass and energy balances are solved by a numerical method. More information about this method can be found in Smit et al. [23] and Noorman et al. [12]. Radial temperature and concentration gradients are neglected, the model is assumed to be pseudo-homogeneous and no heat losses are taken into account. The pressure drop is calculated with the Ergun equation [24], because experiments in a lab-scale reactor have shown that this equation describes the pressure drop well [25]. The model equations are listed in Table 1. In Table 2 the description of the axial mass dispersion and the effective heat conductivity are shown. The thermodynamic properties of the gases and the solids were taken from Daubert and Danner [26] and Barin [27] respectively.

The kinetics from Garcia-Labiano et al. [28] and Zafar et al. [29] have been selected, including the expected influence of diffusion limitations inside the particles, which have been determined with the particle model [30] and are shown in Table 1. The influence of the reaction rate in large packed bed reactors is limited to the shape of the reaction front, which covers only a small part of the reactor. So, as long as the reaction rates are not very slow, the kinetics have a small influence on the outlet temperature and concentration profiles. In fact, the maximum temperature achievable in the packed bed is determined by the active metal in the oxygen carrier, as demonstrated in Equation (2) [10].

$$\Delta T = \frac{(-\Delta H_{R,i})}{\frac{C_{p,s}M_{act}}{\omega^0_{act}\varsigma} - \frac{C_{p,g}M_{g,i}}{\omega^{in}_{g,i}}} \tag{2}$$

In order to reproduce the behavior of the CLC unit after long operating time, sequential simulations have been performed until pseudo-steady state condition was obtained. This was always achieved after three cycles [13]. The results obtained under such conditions are discussed in this work.

[1] The O_2 depleted air from the oxidation stage might be also used for this purpose, with expected minor effects on plant efficiency and avoiding the auxiliary N_2 compressor. The drawback of this option is that such gas may contain some residual oxygen during the breakthrough time at the end of the oxidation stage, that may lead to unwanted gas phase reactions with the syngas inside the reactors and in the gas piping lines right before or after the purging phase.

Table 1
The mass and energy balances used in the model.

Component mass balances for the gas phase

$$\varepsilon_g \cdot \rho_g \frac{\partial \omega_{i,g}}{\partial t} = -\rho_g \cdot v_g \frac{\partial \omega_{i,g}}{\partial x} + \frac{\partial}{\partial x}\left(\rho_g \cdot D_{ax} \frac{\partial \omega_{i,g}}{\partial x}\right) + r_i \cdot M_i$$

Kinetic terms:

Ni and Cu: $r_i = \frac{\varepsilon_s \cdot \varepsilon_{s,p} \cdot \rho_s \cdot \omega^0_{act} \cdot \eta_{effectiveness}}{b \cdot M_j} \frac{dX}{dt}$, (dX/dt from Ref. [28])

Mn: $r_i = \frac{\varepsilon_s \cdot \varepsilon_{s,p} \cdot \rho_s \cdot \omega^0_{act} \cdot \eta_{effectiveness}}{b \cdot M_j \cdot k_0 \cdot \exp\left[\frac{E_A}{R \cdot T}\right]} \pi$, (k0, E_A, n from Ref. [29])

Component mass balance for the solid phase

$$\varepsilon_s \rho_s \omega^0_{act} \frac{\partial \omega_{s,j}}{\partial t} = \varepsilon_g r_j M_j$$

Energy balance (gas and solid phase):

$$(\varepsilon_g \rho_g C_{p,g} + \varepsilon_s \rho_s C_{p,s}) \frac{\partial T}{\partial t} = -\rho_s v_g C_{p,g} \frac{\partial T}{\partial x} + \frac{\partial}{\partial x}\left(\lambda_{ax} \frac{\partial T}{\partial x}\right) + \varepsilon_g r_i \Delta H_{R,i}$$

Effectiveness factors, calculated with particle model [30]

	NiO/Ni	CuO/Cu	Mn_3O_4/MnO
O_2	0.2	0.23	0.66
H_2	0.55	0.53	0.65
CO	0.32	0.36	0.54

3. Results and discussion

3.1. TS-CLC in series or in parallel

For TS-CLC two different configurations can be used. During heat removal both reactors have to be connected in series to transfer the heat generated in the first reactor to the second reactor. But for the reduction and the oxidation mode, the reactors with different oxygen carriers can be connected in series or in parallel. In case the reactors are in series, the gas flows are fed to the first bed and the outlet is fed to the second bed, as illustrated in Fig. 3. With this configuration it is also possible to operate with one reactor that contains two sections (with two different oxygen carriers), because the two stages are always operated in series. This has the advantage of lower complexity of the reactors network.

An alternative is to operate the reactors in parallel during one or both the oxidation and the reduction steps. In those cases, higher flow rates can be used while still complying with the maximum allowable pressure drop because of the reduced reactor length. So, in the end the total cross-section can be reduced. Another advantage is that the CO_2/H_2O is produced at lower temperature in the first reactor increasing the amount of heat stored for the heat removal. The main drawback is that also valves have to be installed downstream of the first reactor and thus, a larger number of valves is required.

Table 2
The heat and mass dispersion descriptions.

Effective axial heat dispersion (Vortmeyer and Berninger [31])

$$\lambda_{ax} = \lambda_{bed,0} + \frac{\mathrm{Re} \cdot \mathrm{Pr} \cdot \lambda_g}{\mathrm{Pe}_{ax}} + \frac{\mathrm{Re}^2 \cdot \mathrm{Pr}^2 \cdot \lambda_g}{6(1-\varepsilon_g)\mathrm{Nu}}$$

$\lambda_{bed,0}$ is calculated by the Bauer and Schlünder equation [32].

Gunn and Misbah equation [33]

$$\mathrm{Pe}_{ax} = \frac{2\left(0.17+0.33 \cdot \exp\left[\frac{-24}{\mathrm{Re}}\right]\right)}{1-\left(0.17+0.33 \cdot \exp\left[\frac{-24}{\mathrm{Re}}\right]\right)}$$

Gunn equation [34]

$$\mathrm{Nu} = (7 - 10\varepsilon_g + 5\varepsilon_g^2)(1 + 0.7\mathrm{Re}^{0.2}\mathrm{Pr}^{1/3}) + (1.33 - 2.4\varepsilon_g + 1.2\varepsilon_g^2)\mathrm{Re}^{0.7}\mathrm{Pr}^{1/3}$$

Axial mass dispersion (Edwards and Richardson [35])

$$D_{ax} = \left(\frac{0.73}{\mathrm{Re} \cdot \mathrm{Sc}} + \frac{0.5}{\frac{9.7\varepsilon_g^2}{\varepsilon_g + \frac{\varepsilon_g}{\mathrm{Re} \cdot \mathrm{Sc}}}}\right) v_g \cdot d_p$$

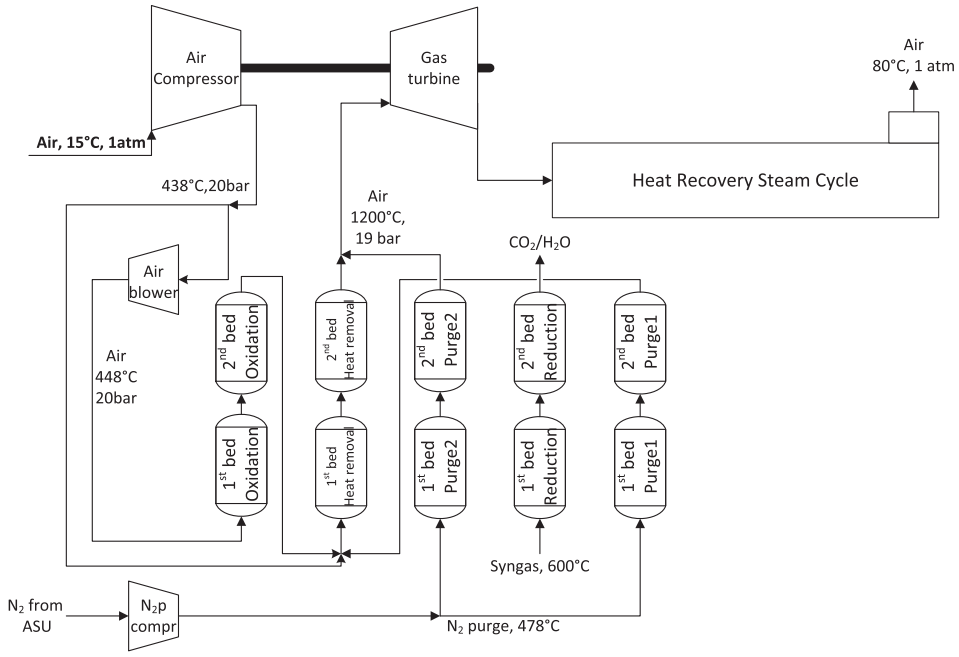

Fig. 3. TS-CLC configuration with all the operation steps in series (TS-CLC series).

In principle, it is possible to operate the reduction, oxidation and the purge in parallel. But in case the oxidation is carried out in parallel, the inlet zone of the second bed is cooled down too much and therefore the gas flow obtained from the heat removal has a lower temperature, which reduces the process efficiency. Therefore, it was chosen to operate only the reduction in parallel. In Fig. 4 it is shown how the process is operated in this case. Because the reactors operate in parallel, more valves are required. The valves for the second beds need to withstand 1200 °C, but the maximum temperature of the valves on the first reactor is lower (around 900 °C).

3.2. Reactor sizing and initial investment cost estimation

For the reactor sizing, a simple cylindrical geometry has been considered for the CLC reactor vessels, featuring an inner diameter D and a length L. A continuous process has been simulated by the 1D reactor model. To design the continuous process, a number of reactors per operation step have to be used and the flow rates have to be calculated. These parameters have been calculated based on the following criteria:

- Two cycle times τ were selected: 20 and 60 min. Such cycle times have been selected as reasonable and representative values, to show how cycle time affects the sizing of the reactors system. An optimization of the cycle time is however beyond the scope of this work, since this should involve an evaluation of the valve lifetime as function of the opening-closure frequency (the shorter the cycle, the higher the opening-closure frequency).
- The pressure drop should not exceed 5% (1 bar); the pressure drop has a large influence on the process efficiency and the number of reactors [8]. A pressure drop of 5% has been selected in this study, but a techno-economic evaluation is required to draw conclusions about this parameter, which is not in the scope of this work.
- The inner reactor diameter is set on 2.5 m in case of a cycle time of 20 min and 4 m for a cycle time of 60 min. In both cases, a similar L/D-ratio is obtained, which makes it justified to compare those cases.
- The total purge size is equal to the total empty volume of the reactor; this should be sufficient, because the gas mixing inside the reactor is very small.

During the cycle (20 or 60 min), sufficient oxygen should be available for the indirect combustion of syngas. So, the total volume V_R of all the reactors together is fixed according to Equation (3). This is based on the oxygen carrier properties ($\rho_{mol,oxygen}$ is the amount of atomic oxygen carried by the oxygen carrier per m^3 reactor, which are listed in Table 3) and results from the material balance stating that the oxygen atoms needed to oxidize the syngas during a complete cycle $(\dot{M}_{CO} + \dot{M}_{H2}) \cdot \tau$ has to equal the oxygen atoms available in the reactors $V_R \cdot \rho_{mol,oxygen}$.

$$V_R = \frac{\left(\dot{M}_{CO} + \dot{M}_{H2}\right) \cdot \tau}{\rho_{mol,oxygen}} \tag{3}$$

For continuous operation, several reactors have to be in operation. The minimum number is five, because there are five operation steps (oxidation, reduction, heat removal and 2 purge steps). For a purge step, only one reactor is used. The criterion to determine the number of reactors is the pressure drop inside the reactors. For a certain reactor length, the maximum specific flow rate $\dot{m}_s$ (kg/(m^2-s) is calculated based on the Ergun equation (Table 1) considering the highest possible gas temperature. With this value, the number of reactors in a certain operation step $N_{R,operation\ step}$ is calculated by rounding up the ratio between the total flow rate $\dot{m}$ by this maximum specific flow rate and the cross section of a reactor (Equation (4)). In this study, the reactor diameter D was fixed at 2.5 or 4 m (dependent on the cycle time) and also the total reactor volume is fixed by the amount of oxygen (Equation (3)). So, the only parameters to be determined are the length L and the total number of reactors N_R (Equation (5)). Both are connected via Equation (6). By varying the length of the reactors, the minimum number of reactors allowing not to exceed the imposed pressure drops limit can be found. In other words, given τ, D, $\rho_{mol,oxygen}$ and $\dot{m}$, the

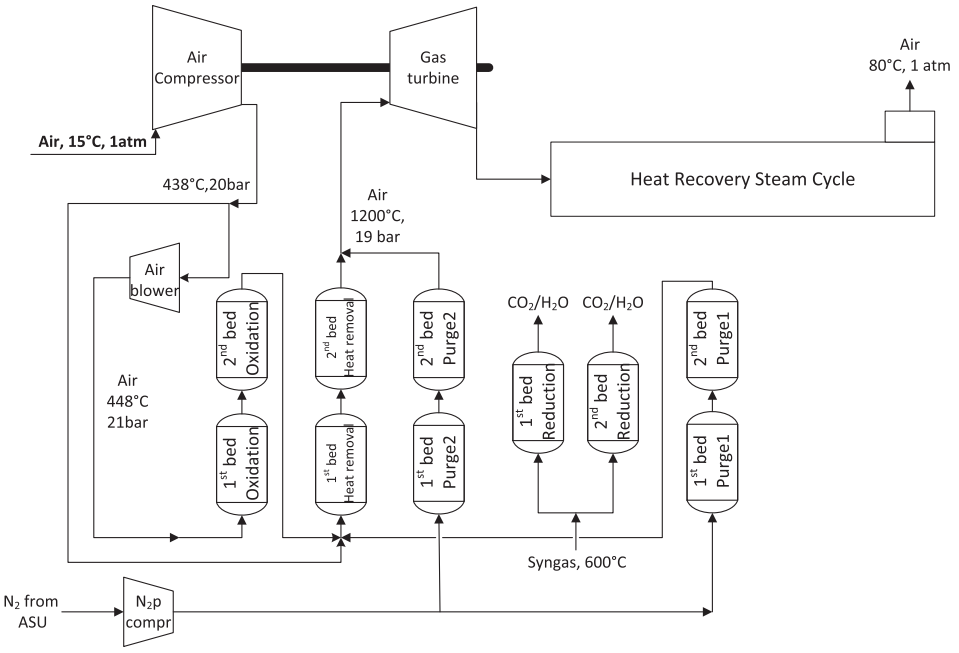

Fig. 4. TS-CLC configuration with the reduction in parallel and the other operation steps in series (referred as: TS-CLC parallel).

unknowns V_R, $N_{R,operation\ step}$, N_R, L and $\dot{m}_s$ can be found through Equations (3)–(6) and the Ergun equation.

$$N_{\mathrm{R,operation\ step}} = \mathrm{ceil}\left(\frac{\dot{m}}{\dot{m}_s \cdot \pi/4 \cdot D^2}\right) \tag{4}$$

$$N_R = \sum_{i=1}^{\text{total number of operation steps}} N_{\mathrm{R,operation\ step}} \tag{5}$$

$$V_R = N_R \cdot \pi/4 \cdot D^2 \cdot L \tag{6}$$

Clearly, the total reactor volumes are based on the properties of the selected oxygen carriers. For the one stage case, 19 wt% of NiO/Al_2O_3 is sufficient to reach 1200 °C in the reactors. The active weight contents for the TS-CLC cases are also based on this outlet temperature. In the TS-CLC cases, the heat removal gas inlet temperature is different, so a different ΔT has to be reached and therefore both cases have a different active weight content. Based on the active weight contents and the density, the amount of available oxygen per m^3 reactor is calculated (assuming a reduction to Cu, Ni and MnO respectively [13]). As shown in Table 3, the result is that the amount of oxygen carried by a given volume of supported metal is smaller for the TS-CLC configurations. Therefore, a larger reactor volume (about two times larger) is required for those cases for a given cycle time.

The following designs were made for a cycle time of 60 min. For the one stage process, the reactor length is 11.8 m and there are 24 reactors in operation. For TS-CLC in series the total length is 22.5 m (bed 1: 12 m and bed 2: 10.5 m), while there are 27 reactors (54 beds in total) in operation. These bed sizes were selected to keep the difference between the minimum and the maximum temperature in each reactor as small as possible and thus the total ΔT as small as possible. This has the advantage that the oxygen carrier particles experience the lowest possible thermal stress, which can be advantageous for the mechanical stability and possibly increase its lifetime. For the TS-CLC in parallel, the first reactor is 12 m and the second is 11.5 m and there are 50 reactors in total. An overview of the sizing parameters can be found in Table 4.

TS-CLC series is considered to be carried out in one reactor of 22.5 m that contains two sections. In that case, the footprint is 340 m^2. If the process is operated in two separate reactors both placed at the ground level, the total footprint would be a factor 2 larger. TS-CLC parallel has to be carried out in two separate reactors, because the reduction is carried out in parallel and therefore a larger total footprint is required, 628 m^2.

Table 4 also contains the sizing of the reactors in the case of a cycle time of 20 min. This option has been designed to evaluate the effect of the cycle time on the initial investment costs.

A preliminary investment cost estimation has been also carried out for the CLC reactors systems, with the aim of comparing just the initial costs of the different types of packed bed CLC configurations. The initial investment costs have been estimated based on the costs of the oxygen carrier, the high temperature valves and the reactors. The reactor containing the oxygen carrier is surrounded by an

Table 3
Properties of the oxygen carriers.

	One stage CLC	TS-CLC series		TS-CLC parallel	
		Bed 1	Bed 2	Bed 1	Bed 2
Oxygen carrier	19wt% NiO/Al_2O_3	10wt% CuO/Al_2O_3	27wt% Mn_3O_4/Al_2O_3	10wt% CuO/Al_2O_3	30wt% Mn_3O_4/Al_2O_3
Oxidation/reduction couple	NiO/Ni	CuO/Cu	Mn_3O_4/MnO	CuO/Cu	Mn_3O_4/MnO
Solids bulk density in oxidized state, $\varepsilon_s\rho_s$ kg/m^3	1031	989	1000	989	1006
Particle diameter, mm	10	10	10	10	10
Void fraction, $m^3_{gas}/m^3_{reactor}$	0.4	0.4	0.4	0.4	0.4
Amount of oxygen available, $kg_{O2}/m^3_{reactor}$	42.0	19.9	18.9	19.9	21.1

Table 4
The sizing parameters for the different reactor concepts.

	One stage CLC		TS-CLC series		TS-CLC parallel	
Cycle time, min.	20	60	20	60	20	60
Number of reactors	35	24	44	27	42x2	25x2
Diameter, m	2.5	4	2.5	4	2.5	4
Length, m	6.9	11.8				
- bed 1, m			6.6	12.5	6.2	12
- bed 2, m			5.2	10	5.8	11.5
Footprint, m^2	172	302	216	340	412	628
Total reactors volume, m^3	1185	3559	2533	7634	2460	7383

internal refractory, a carbon steel vessel and an external refractory. The internal refractory is required to keep the steel vessel temperature below 300 °C. The thickness of the internal refractory and the steel vessel is reported in Table 5. The high temperature refractory thickness $(D_a-D)/2$ is calculated by Equation (7), fixing a maximum reactor temperature $T_{max,CLC}$ of 1200 °C, a steel temperature T_{steel} of 300 °C and a heat flux Q corresponding to the assumed heat loss of 0.25% of the LHV (low heating value) of the CLC fuel. With this assumption the heat losses are in line with a heat transfer from the external surface (at 70 °C) to the environment with a typical heat transfer coefficient of 5 W/(m^2·K) [36]. The heat conductivity of internal insulation material (internal refractory) is 0.2 W/(m·K). For the steel thickness in meter, Equation (8) has been used, in which a design pressure P_{in} of 30 bar is assumed for safety reasons and the design stress, f, is estimated at 85 N/mm^2 [37].

$$Q = \frac{2\pi\lambda_r L}{\ln\left(\frac{D_a}{D}\right)}\left(T_{\max,CLC} - T_{steel}\right) \tag{7}$$

$$\text{steel vessel thickness} \geq \frac{P_{in}D_a}{4f - 1.2P_{in}} \tag{8}$$

The costs of the vessels are calculated considering the steel costs of 500 €/ton [38] and fire bricks (refractory) of 450 €/ton (density of 480 kg/m^3 [39]) and multiply them by a factor 3 to include the reactor construction cost. The cost of a high temperature valve is estimated at € 150,000 in case of a hot gas flow rate (during the heat removal step) of 2 m^3/s. The valve cost is scaled up by Equation (9) [40]. An overview of the high temperature valve system costs for each case is given in Table 5. In case of TS-CLC parallel, the outlet stream of the first reactor has to be managed and thus two valves per set of reactors are required. In the TS-CLC series, this is not required, because the outlet of the first reactor is always going to the second reactor in series. The nickel based carrier costs are estimated at 50,000 €/ton, while the cheaper copper- and manganese-based oxygen carriers that are used for the TS-CLC process are estimated at 10,000 €/ton. All the assumptions for the estimation of the reactors equipment cost and the main results are resumed in Table 5.

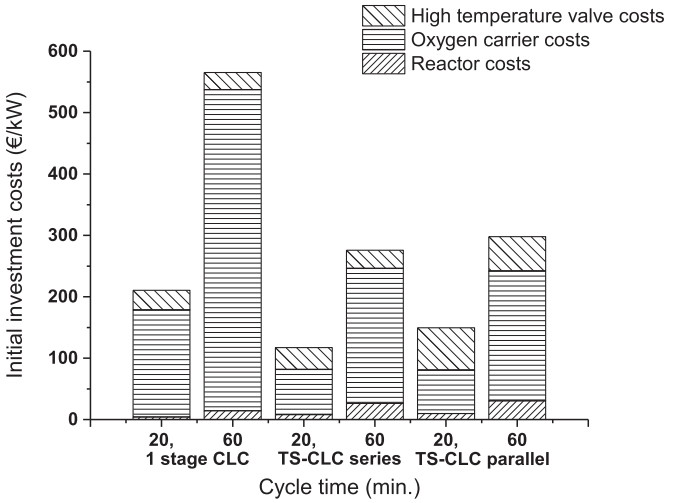

Fig. 5. Initial investment costs for the TS-CLC cases in comparison with the one stage CLC for two different cycle times (20 min and 60 min).

$$C = C_0 \left(\frac{\dot{V}}{\dot{V}_0}\right)^{0.6} \tag{9}$$

In Fig. 5 it is demonstrated that the resulting initial investment costs are about a factor 2 lower in the TS-CLC cases in comparison with the one stage CLC with a nickel-based oxygen carrier, because

Table 5
The sizing parameters for the different reactor concepts.

Assumptions						
Heat losses, Q	0.25% of LHV of the CLC fuel					
Heat conductivity of insulation material	0.2 W/(m·K)					
Heat transfer coefficient between the outer wall and the environment	5 W/(m^2·K)					
Design pressure, P_{in}	30 bar					
Design stress, f	85 N/mm^2					
Steel vessel temperature	300 °C					
Steel cost	500 €/ton					
High temperature refractory cost	450 €/ton					
High temperature refractory density	480 kg/m^3					
High temperature valve cost	150,000 € for 2 m^3/s gas flow					
Ni-based oxygen carrier cost	50,000 €/ton					
Cu and Mn-based oxygen carrier cost	10,000 €/ton					
Results	One stage CLC		TS-CLC series		TS-CLC parallel	
Cycle time, min.	20	60	20	60	20	60
Inner refractory thickness, mm	250	476	237	452	252	484
Steel thickness, mm	27	44	27	44	27	44
Reactor costs, k€ per reactor unit[a]	44	210	64	334	80	424
High temperature valve cost, k€/valve	319	400	278	373	286	390
Number of valves per reactor unit[a]	1		1		2	
Oxygen carrier cost per reactor unit[a], M€	1.75	7.64	0.58	2.81	0.59	2.95
Total cost per reactor unit[a], M€	2.11	8.25	0.92	3.52	1.24	4.15
Total cost of CLC reactor system, M€	73.8	198	40.4	95.0	52.0	104

[a] The single reactor for the single stage CLC and one couple of reactors with the two oxygen carriers for the TS-CLC are intended as reactor unit.

Table 6
Settings for the one stage CLC. The outlet temperatures are results from the packed bed model.

Step	Reactors	Time, s	Mass flux, kg/m^2/s	T_{in}, °C	$T_{out,\ avg}$, °C
Reduction	5	750	1.841	600	832
Purge1	1	150	0.746	478	527
Oxidation	4	600	3.520	448	575
Heat Removal	13	1950	4.311	459	1199
Purge2	1	150	0.746	478	1192
	24	3600			

cheaper oxygen carriers can be used in the TS-CLC cases. The TS-CLC parallel case is slightly more expensive than the TS-CLC series case, because more high temperature valves are required. The purpose of this work is just to demonstrate the effect of the TS-CLC configuration and therefore the economic optimization is not carried out. Such an economic evaluation should include the optimization of the reactor geometry and the effect in the operating costs of the plant, which is out of scope of this work.

Due to the high impact of the oxygen carrier in the investment, the operating cost related with the substitution of the material is expected to be higher for the cost of one-stage CLC plant. So, if the operating costs are considered, the TS-CLC seems to be more attractive despite the higher costs for the reactors network that are expected.

For the process simulation of the reactors, the case with a cycle time of 1 h has been selected to decrease the switching frequency of the high temperature valve at the exit of the reactor to increase its lifetime.

3.3. One stage CLC

Based on the above mentioned criteria, simulations were carried out with the settings shown in Table 6. In total 24 reactors are in operation in this configuration, where 5 reactors are in the reduction step, 4 in oxidation, 13 in heat removal and 1 per purge step. The outlet temperature and mass flux for one reactor as a function of time has been published elsewhere [8].

The axial temperature profiles corresponding to the outlet profile are provided in Fig. 6. It is shown that when the reduction is started, the outlet of the reactor is still hot from the previous heat removal step. This heat is blown out of the bed during the reduction and therefore a decreasing CO_2/H_2O outlet temperature is observed. During the reduction reaction, the temperature inside the reactor is 450–550 °C. In this temperature range, the selectivity of the reduction reactions with nickel (to CO_2 and H_2O) is not a problem according to the thermodynamics. Hence, complete conversion of the fuel is assumed. During oxidation, the temperature of the bed increases to 1200 °C, because of the exothermic reaction. Subsequently, the heat is blown as hot gas stream to the gas turbine (heat removal step).

Several reactors operate during the reduction and the heat removal, which deliver streams at different temperatures. These streams are mixed and then an outlet temperature is obtained as shown in Fig. 7 [8]. The temperature of the CO_2/H_2O stream fluctuates between 750 and 900 °C with an average temperature of 832 °C. These temperature variations might require to be controlled as previously mentioned to protect the downstream heat exchangers. Such mixed stream, considered at its average

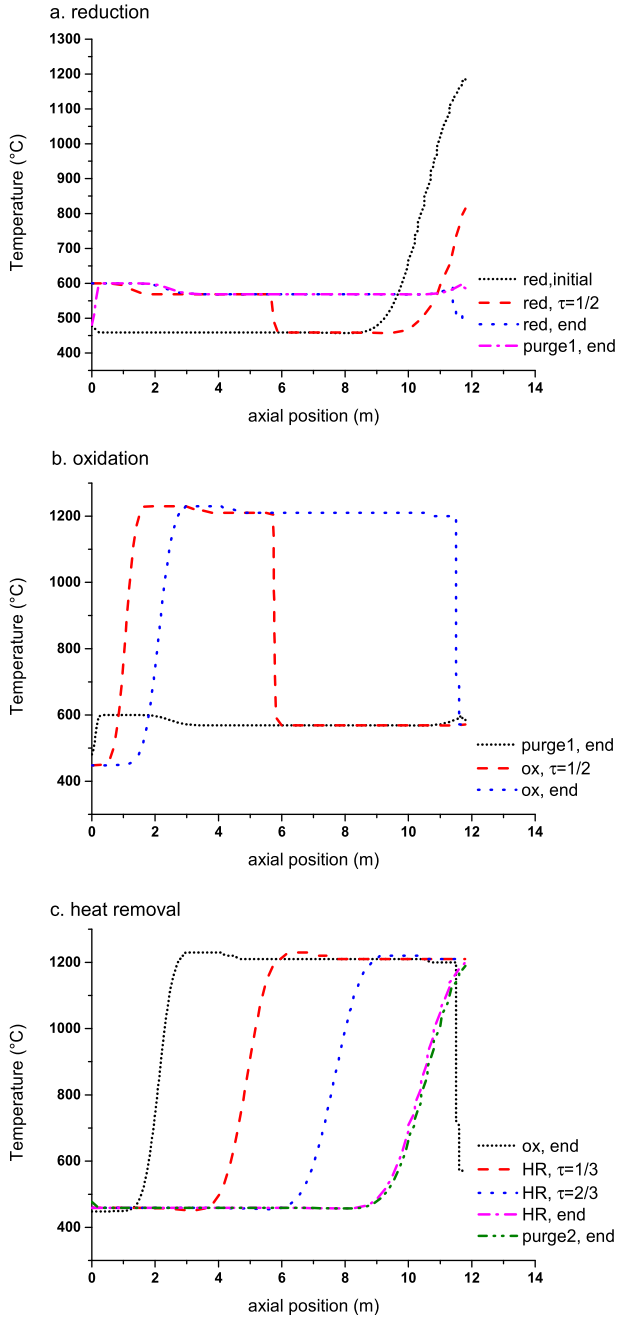

Fig. 6. Axial temperature profiles of reactors in the one stage CLC process during reduction (a), oxidation (b) and heat removal (c).

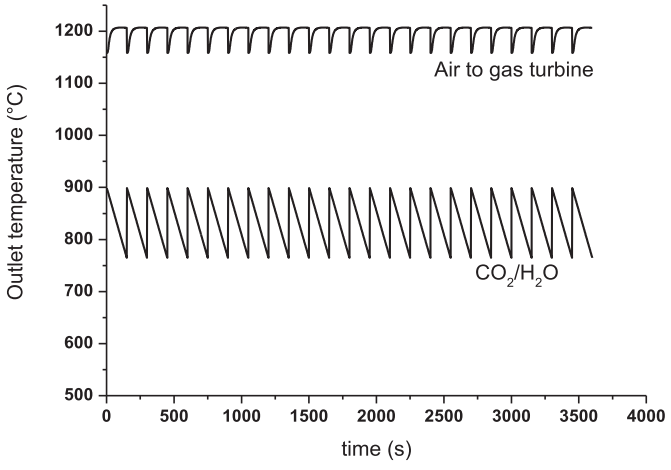

Fig. 7. Outlet temperature during dynamic operation of reactors in the one stage CLC process [8].

Table 7
Simulation settings for TS-CLC in series.

Step	Reactors	Time, s	Mass flux, kg/m^2/s	T_{in}, °C	$T_{out,\ avg}$, °C
Reduction	3	400	3.068	600	1130
Purge1	1	133	1.569	478	1032
Oxidation	5	667	2.815	449	970
Heat Removal	17	2267	2.856	574	1198
Purge2	1	133	1.569	478	1202
	27	3600			

temperature in the power plant process simulations, is sent to a heat exchanger, where high pressure steam is generated at 565 °C.

After integrating the obtained streams from the reactor model within the power plant model, mass and energy balances are obtained. With this process, a net electric efficiency of 41.05% can be achieved. An overview of the energy balance is given in section 3.6, which shows the electricity production and consumption in the power plant.

3.4. TS-CLC series

The same procedure has been carried out for the option in which TS-CLC is carried out with two reactors in series. This reactor is simulated as one large reactor that consists of two beds. The first bed (with CuO/Al_2O_3) has a length of 12.5 m and the second bed (with Mn_3O_4/Al_2O_3) has a length of 10 m (from 12.5 to 22.5 m). The simulation settings are listed in Table 7. The inlet temperature for the heat removal is higher than in the one stage case (574 °C instead of 459 °C), due to the mixing with the gas streams from at the outlet of oxidation and purge1 which are at higher temperature respect to one-stage CLC. As is illustrated in Fig. 8, a constant air flow at 1200 °C can also be produced with this configuration.

During reduction, CO_2 and H_2O are produced at a higher temperature than in the one stage case, caused by the increased heat dispersion in the packed bed due to the two stage operation [13]. The larger extent of heat dispersion can be explained as follows. The extent of heat dispersion in the first bed is similar to the one stage configuration. But in this case, the dispersed gas flow obtained from the first reactor is sent to the second reactor, where it experiences some additional heat dispersion. In Fig. 9 the axial temperature profiles inside the reactor are shown. During reduction, syngas is fed at 600 °C and the temperature in the CuO-reactor rises due to the exothermic reduction reactions. In the Mn_3O_4-reactor, the temperature rise is smaller, because the reduction reactions are less exothermic. When the reduction is completed, two different temperature plateaus can be observed: the first reactor is mainly at 700 °C and the second reactor mainly at 900 °C. During oxidation, air is fed at only 448 °C and therefore a temperature drop can be observed at the inlet of the first reactor. Due to the exothermic oxidation reaction, the temperature rises by about 200 °C in the first reactor and 300 °C in the second reactor, so that a 1200 °C plateau is reached in the second reactor. After the bed has been oxidized, the heat is blown out of the bed and a continuous flow of air at 1200 °C is produced. The average outlet temperatures are shown in Fig. 10. In this case, the CO_2/H_2O stream is produced at a higher temperature than in the one stage CLC case and also the temperature fluctuations are smaller (30 °C instead of 140 °C).

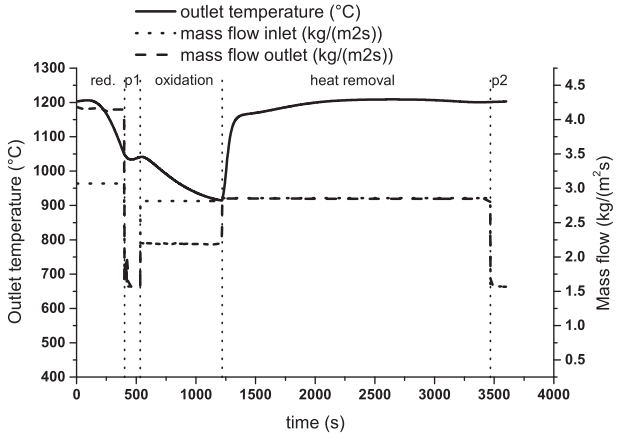

Fig. 8. The outlet temperature and mass flux profile from TS-CLC with the two reactors always connected in series.

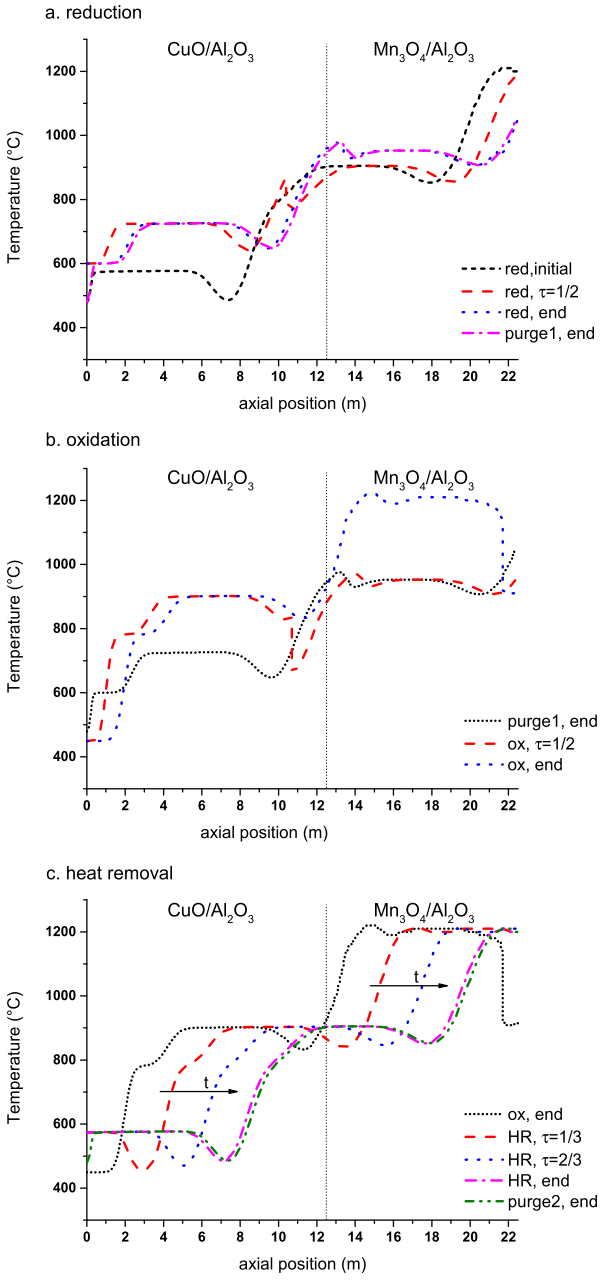

Fig. 9. Axial temperature profiles during TS-CLC, for the case where the reactors are always connected in series.

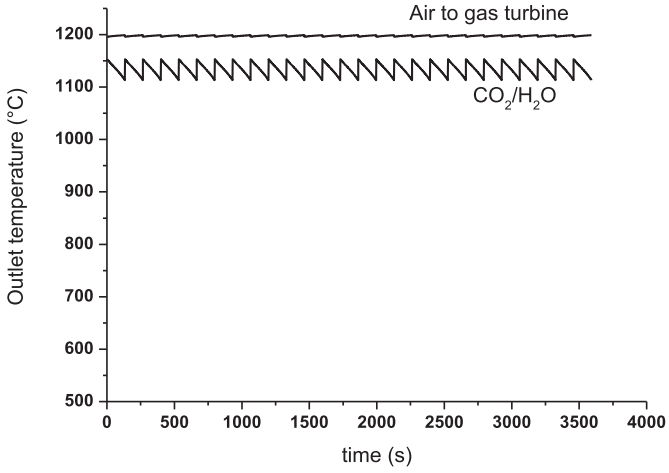

Fig. 10. Average outlet temperatures from the TS-CLC series process.

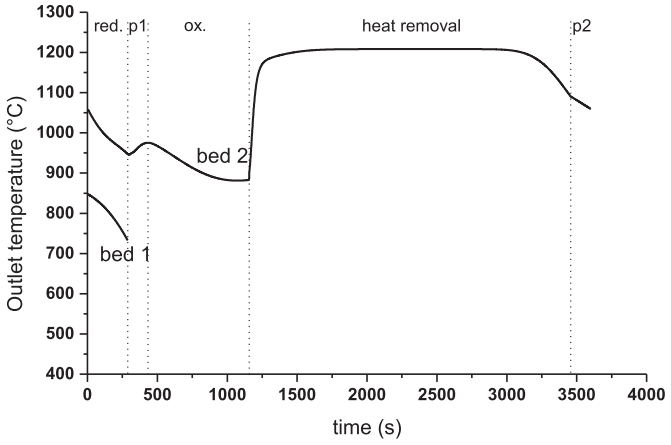

Fig. 11. Outlet temperatures from the first and second reactor that are processed downstream.

The axial temperature profiles from Fig. 9 show the reduced temperature difference among the different steps compared to the one stage CLC operation. In the first bed, a maximum ΔT of less than 500 °C is observed. The minimum temperature in the second reactor is at around 850 °C during the oxidation, resulting in a maximum ΔT of 350 °C.

3.5. TS-CLC with reduction in parallel (TS-CLC parallel)

As explained before, it is also possible to operate CLC in two stages with the reduction in parallel to produce CO_2 at lower average temperatures.

The two reactors used for this configuration are simulated separately. The simulation settings are shown in Table 8. The outlet temperature profiles of the streams that are processed downstream are shown in Fig. 11. Also in this case, a gas stream with a constant temperature of 1200 °C is obtained during heat removal from the second reactor.

In Fig. 11, it is shown that the temperature decrease during the reduction is smaller than in the one stage configuration. In total, 4 parallel reduction reactors are in operation, whose streams are mixed before being sent to the heat recovery section. This mixed stream has smaller temperature differences and this is an advantage for the design of the downstream heat exchanger. The axial temperature profiles are shown in Fig. 12. The first reactor looks similar to the one stage case; only the temperature levels are different (related to the different oxygen carrier used). However, profiles in the second reactor are significantly different from the profiles in the other two cases. Before the reduction starts, a large part of the reactor has a temperature of 850 °C. During the reduction step, syngas is fed into the reactor at 600 °C and CO_2/H_2O is produced at 1050–950 °C. During oxidation, a heat plateau is formed at 1200 °C. This heat is blown out of the bed during the heat removal step. Feeding the second reactor with relatively cold syngas at 600 °C, leads to a significant temperature drop at the inlet. This leads to an irregular temperature profile for the following stages, with an area with local maximum and local minimum temperature which is progressively blown to the exit of the reactor. However, thanks to the heat diffusion in the axial direction, the temperature profile becomes more uniform during the heat removal phase and the temperature of the hot gases produced is sufficiently stable to feed the power cycle.

In Fig. 12 it is shown that the maximum temperature difference that the reactors experience, is limited in the first reactor (between 450 and 500 °C, as in the TS-CLC series case), but relatively large in the second reactor (600 °C). A larger ΔT is observed in the second reactor, because the fuel is fed at 600 °C and air is produced at 1200 °C.

When mixing the gases produced by reactors operating in parallel during the same stage, the averaged outlet temperature profiles illustrated in Fig. 13 are obtained.

3.6. Comparison of the different configurations

For each of the three configurations, the integration in the power plant has been designed and the efficiency evaluated. The mass balances for the three configurations are shown in Table 9. If CO_2 and H_2O are produced at a higher temperature (#2), more high pressure steam is produced in the downstream cooler. For this reason, the amount of high pressure steam (#13) in the TS-CLC series case differs significantly from the other cases. When more energy is taken by the CO_2/H_2O stream and therefore more power is produced in the steam turbine, less power is produced in the gas turbine as a consequence of the lower air flow rate obtained from the heat removal (#10). The superheated and reheated steam temperature in the HRSG is about 25 °C below the turbine outlet temperature (#11).

Table 8
Simulation settings for TS-CLC with reduction in parallel and oxidation, heat removal and purges in series (TS-CLC parallel).

Step	Reactors	Time, s	Mass flux, kg/m^2/s	T_{in}, °C	$T_{out,\ avg}$, °C
Reduction reactor 1	2	288	2.233	600	801
Reduction reactor 2	2	288	2.369	600	994
Purge1	1x2	144	1.521	478	962
Oxidation	5x2	720	2.816	448	915
Heat Removal	16x2	2304	3.393	547	1192
Purge2	1x2	144	1.521	478	1075
	25x2	3600			

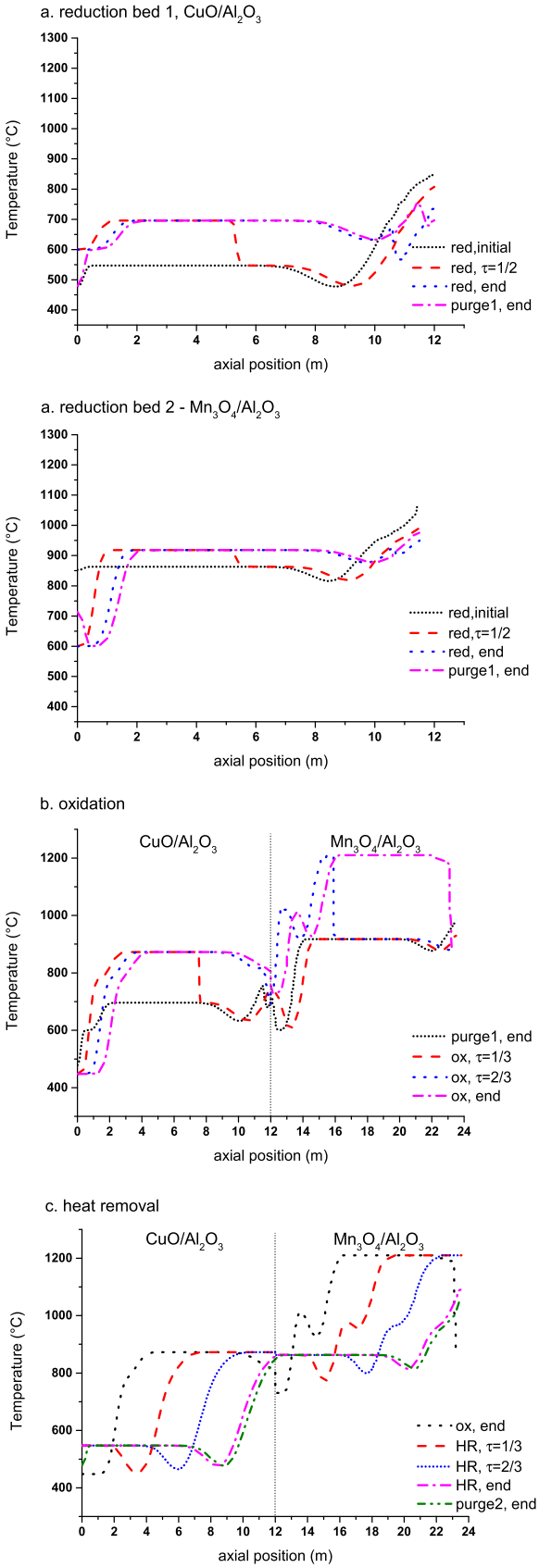

Fig. 12. Axial temperature profiles during TS-CLC with the reduction in parallel.

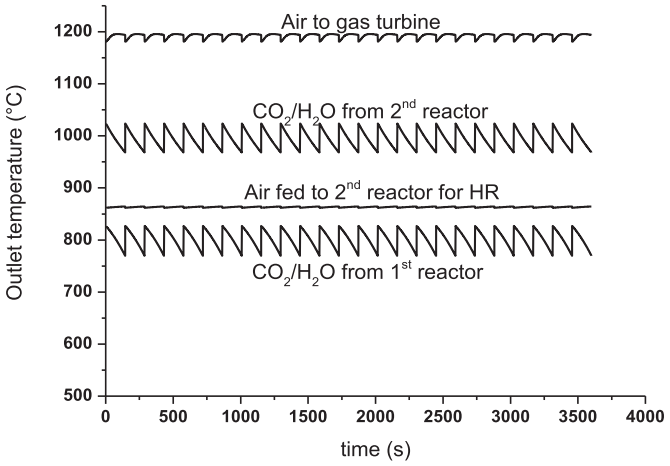

Fig. 13. Outlet temperature profiles from the parallel TS-CLC.

The energy balances of the three configurations are listed in Table 10, including in the first two columns a reference IGCC (integrated gasification combined cycles) plant without CO_2 capture and with conventional capture with Selexol [2]. These configurations are based on current technology. The CO_2 avoided and the specific primary energy consumption for CO_2 avoided (SPECCA) [41] are calculated by Equations (10) and (11) with the IGCC plant without CO_2 capture as reference.

$$CO_{2,\text{avoided}} = 1 - \frac{E_{CO_2}}{E_{CO_{2,\text{ref}}}} \tag{10}$$

$$\text{SPECCA} = \frac{\frac{1}{\eta_{el}} - \frac{1}{\eta_{el,ref}}}{E_{CO2,ref} - E_{CO2}} 3600 \tag{11}$$

In the one stage case, the highest LHV efficiency is obtained, 41.05%, but the TS-CLC cases can still compete well with the one stage case, with efficiencies of 40.34–40.77%. In the TS-CLC series configuration, a larger amount of high pressure steam is produced and this results in a larger electricity production by the steam cycle and a lower output from the gas turbine. A slightly higher LHV efficiency can be obtained in the TS-CLC parallel case (40.77%) compared with TS-CLC series (40.34%), because of the lower CO_2 temperature. In all the IG-CLC cases, the efficiency is more than 5% points higher than the reference case with Selexol. The CLC cases also have lower specific CO_2 emissions (reduced by a factor four) and a lower electricity consumption for CO_2 capture (SPECCA) (by factor three) than the plant with conventional CO_2 capture.

As far as “classical” pollutant emissions are concerned, virtually no NO_x and SO_x emissions are foreseen for the CLC-based processes with respect to the conventional Selexol-based capture plant. As a matter of fact, the lack of a direct contact air-fuel combustion will avoid the formation of thermal NO_x, which might be of particular concern in case of a H_2-fuel based flame. Also for SO_x, it can be anticipated that any H_2S escaping form the sulfur removal unit will be oxidized by the oxygen carrier, likely resulting in traces of SO_2 in the final compressed CO_2. On the other hand, particulate emissions might derive from the oxygen carrier fragmentation, which should be avoided by developing materials with a proper mechanical stability to thermal and mechanical cycles. Also from this side, the higher flexibility in the oxygen carrier selection represents an advantage of the TS-CLC process.

Table 9
The mass balances of the three different packed bed configurations.

#		One stage CLC (base case)			TS-CLC series			TS-CLC parallel		
		T,°C	p,bar	M,kg/s	T,°C	p,bar	M,kg/s	T,°C	p,bar	M,kg/s
1	Syngas	600	20.0	116.3	600	20.0	116.3	600	20.0	116.3
2	CO_2/H_2O	832	19.0	156.9	1130	19.0	156.9	901[a]	19.0	156.9
3	CO_2/H_2O	136	18.0	156.9	127	18.0	156.9	136	18.0	156.9
4	CO_2	28	110.0	81.5	28	110.0	81.5	28	110.0	81.5
5	Air	15	1.0	786.2	15	1.0	668.3	15	1.0	750.8
6	Air	438	20.0	729.8	438	20.0	617.6	438	20.0	696.8
7	Air	448	21.0	176.6	449	21.0	176.6	448	21.0	176.6
8	O_2 depl. Air	466	20.0	698.4	586	20.0	596.8	554	20.0	675.3
9	N_2	478	20.4	18.4	478	20.4	39.5	478	20.0	38.2
10	O_2 depl. Air	1199	19.0	707.6	1198	19.0	616.5	1192	19.0	694.4
11	O_2 depl. Air	486	1.0	764.0	482	1.0	667.2	482	1.0	748.4
12	O_2 depl. Air	92	1.0	764.0	81	1.0	667.2	89	1.0	748.4
13	Steam	565	133.9	88.6	565	133.9	130.6	565	133.9	98.0
14	Steam	527	133.9	129.5	544	133.9	157.4	530	133.9	136.3
15	Steam	333	36.0	129.5	346	36.0	157.4	335	36.0	136.3
16	Steam	458	33.1	142.6	453	33.1	161.3	453	33.1	147.1
17	Steam	395	21.6	33.4	390	21.6	33.4	390	21.6	33.4
18	Steam	300	3.5	37.7	300	3.5	30.9	300	3.5	36.1
19	Steam	32	0.05	146.8	32	0.05	158.7	32	0.05	149.8
Maximum ΔT in CLC reactors, °C		760			500/350			450/600		
Maximum ΔT after mixing the CO_2/H_2O flows, °C		140			30			50		

[a] both CO_2/H_2O streams are considered to be mixed.

Table 10
Energy balances of the different configurations.

Power	IGCC-NC N/A [2]	IGCC Selexol® [2]	One stage CLC	TS-CLC series	TS-CLC parallel
Heat input LHV, MW_{LHV}	812.5	898.8	853.9	853.9	853.9
Gas turbine, MW_e	261.6	263.9	225.1[a]	194.0[a]	217.3[a]
Heat Recovery Steam Cycle, MW_e	179.5	161.2	183.0	208.1	188.3
Gross power output, MW_e	441.1	425.1	408.1	402.1	405.6
Syngas blower, MW_e	−1.0	−1.1	−0.8	−0.8	−0.8
N_2 compressor, MW_e	−34.1	−29.8			
ASU, MW_e	−29.6	−32.7	−33.9	−33.9	−33.9
Lock hoppers CO_2 compressor, MW_e			−3.1	−3.1	−3.1
Acid Gas Removal, MW_e	−0.4	−14.7	−0.4	−0.4	−0.4
CO_2 compressor, MW_e		−19.7	−11.0	−11.0	−11.0
Heat rejection, MW_e	−5.5	−6.3	−3.6	−3.8	−3.7
Other auxiliaries, BOP, MW_e	−3.2	−3.6	−4.7	−4.7	−4.7
Net power generated, MW_e	367.4	317.3	350.6	344.5	348.1
LHV efficiency, %	45.21	35.31	41.05	40.34	40.77
CO_2 capture efficiency, %		89.8	97.1	97.1	97.1
CO_2 purity, %		98.2	96.7	96.7	96.7
CO_2 emission, kg CO_2 emitted/MWh_e	769.8	101.4	24.7	25.1	24.9
CO_2 avoided, %	0	86.8	96.8	96.7	96.8
SPECCA, MJ LHV/kg CO_2		3.34	1.08	1.29	1.16

[a] Gas turbine power includes consumption of air blower and nitrogen compressor for purge.

4. Conclusions

The performances of different packed bed CLC configurations in an IGCLC power plant have been compared based on process and reactor design and the initial investment costs. In one stage packed bed CLC, the temperature increase during the oxidation step is achieved in a single stage by means of a single oxygen carrier. Recently, a different approach has been demonstrated in which temperature increase is achieved in two stages (TS-CLC) by means of two oxygen carriers. In this case, during the heat removal operation step, heat is blown from the first bed to the second bed and from the second bed to the gas turbine. In this step, both reactors need to be connected in series. But the oxidation, reduction and purge steps can also be operated with both reactors in parallel.

In this work, it has been demonstrated that with the TS-CLC system based on Cu and Mn based oxygen carriers, a LHV efficiency close to the one stage CLC can be reached (40.3–40.8% compared to 41.1%). For TS-CLC a larger reactor volume is needed, because a lower temperature change per reactor is desired. The lower temperature change is possible if the oxygen content of the oxygen carrier material is decreased and this leads to a larger total reactor volume. Despite the larger reactor volume, the initial investment costs for TS-CLC are estimated to be a factor two smaller, because of the lower costs for the oxygen carrier.

If TS-CLC with series and parallel fuel feeding are compared, parallel feeding shows higher efficiency but also higher investment cost, mainly due to the need of a larger number of high temperature valves. Therefore, further investigation with more reliable cost functions is needed to understand which of the two TS-CLC options is the most profitable.

Other issues will have to be considered when comparing the one stage and the two-stage CLC systems, e.g. stability over time, reliability, controllability, which should be evaluated based on

experimental work. This study has however demonstrated that, despite the slightly lower process efficiency, TS-CLC based on Cu−Mn oxygen carriers allows reducing significantly the cost of the CLC reactor system, and may hence be preferable on the economic side. The larger flexibility in the selection of the oxygen carriers is an intrinsic advantage of this system, which can be decisive in designing cheaper and high efficiency CLC processes.

Acknowledgments

The research originating these results has been supported by the CATO-2 program under the project number WP1.3F2.

References

[1] Erlach B, Schmidt M, Tsatsaronis G. Comparison of carbon capture IGCC with pre-combustion decarbonisation and with chemical-looping combustion. Energy 2011;36:3804−15.
[2] Spallina V, Romano MC, Chiesa P, Gallucci F, Van Sint Annaland M, Lozza G. Integration of coal gasification and packed bed CLC for high efficiency and near-zero emission power generation. Int J Greenh Gas Control 2014;27: 28−41.
[3] Adanez J, Abad A, Garcia-Labiano F, Gayan P, de Diego LF. Progress in chemical-looping combustion and reforming technologies. Prog Energy Combust Sci 2012;38:215−82.
[4] Gayán P, Abad A, de Diego LF, García-Labiano F, Adánez J. Assessment of technological solutions for improving chemical looping combustion of solid fuels with CO_2 capture. Chem Eng J 2013;233:56−69.
[5] Cormos C-C. Evaluation of syngas-based chemical looping applications for hydrogen and power co-generation with CCS. Int J Hydrogen Energy 2012;37: 13371−86. http://dx.doi.org/10.1016/j.ijhydene.2012.06.090.
[6] Rezvani S, Huang Y, McIlveen-Wright D, Hewitt N, Mondol JD. Comparative assessment of coal fired IGCC systems with CO_2 capture using physical absorption, membrane reactors and chemical looping. Fuel 2009;88: 2463−72.
[7] Sorgenfrei M, Tsatsaronis G. Design and evaluation of an IGCC power plant using iron-based syngas chemical-looping (SCL) combustion. Appl Energy 2013;113:1958−64.
[8] Hamers HP, Romano MC, Spallina V, Chiesa P, Gallucci F, Van Sint Annaland M. Comparison on process efficiency for CLC of syngas operated in packed bed and fluidized bed reactors. Int J Greenh Gas Control 2014;28:65−78. http://dx.doi.org/10.1016/j.ijggc.2014.06.007.
[9] Consonni S, Lozza G, Pelliccia G, Rossini S, Saviano F. Chemical-looping combustion for combined cycles with CO[sub 2] capture. J Eng Gas Turbines Power 2006;128:525. http://dx.doi.org/10.1115/1.1850501.
[10] Naqvi R, Bolland O. Multi-stage chemical looping combustion (CLC) for combined cycles with CO_2 capture. Int J Greenh Gas Control 2007;1:19−30.
[11] Noorman S, Gallucci F, Van Sint Annaland M, Kuipers JAM. Experimental investigation of chemical-looping combustion in packed beds: a parametric study. Ind Eng Chem Res 2011;50:1968−80.
[12] Noorman S, Van Sint Annaland M, Kuipers JAM. Packed bed reactor technology for chemical-looping combustion. Ind Eng Chem Res 2007;46:4212−20.
[13] Hamers HP, Gallucci F, Cobden PD, Kimball E, Van Sint Annaland M. A novel reactor configuration for packed bed chemical-looping combustion of syngas. Int J Greenh Gas Control 2013;16:1−12.
[14] Spallina V, Gallucci F, Romano MC, Chiesa P, Lozza G, Van Sint Annaland M. Investigation of heat management for CLC of syngas in packed bed reactors. Chem Eng J 2013;225:174−91.
[15] GECOS. GS software. 2013. doi: www.gecos.polimi.it/software/gs.php.
[16] Lozza G. Bottoming steam cycles for combined gas-steam power plants. A theoretical estimation of steam turbine performances and cycle analysis. In: Proc. 1990 ASME Cogen-Turbo, New Orleans (USA); 1990. p. 83−92.
[17] Chiesa P, Macchi E. A thermodynamic analysis of different options to break 60% electric efficiency in combined cycle power plants. J Eng Gas Turbines Power 2004;126:770−85.
[18] Gardiner WC. Combustion Chemistry. New York: Springer-Verlag; 1984.
[19] Stull DR, Prophet H. JANAF Thermochemical tables. 2nd ed. Washington,DC: U.S. National Bureau of Standards; 1971.
[20] Schmidt E. Properties of water and steam in S.I. Units. Berlin: Springer-Verlag; 1982.
[21] EBTF, Anantharaman R, Bolland O, Booth N, van Dorst E, Ekstrom C, et al. European best practice guidelines for assessment of CO_2 capture technologies. 2011. www.gecos.polimi.it/research/EBTF_best_practice_guide.pdf.
[22] Aspen Technology Inc. Aspen plus 7.3.2. 2011.
[23] Smit J, Van Sint Annaland M, Kuipers JAM. Grid adaptation with WENO schemes for non-uniform grids to solve convection-dominated partial differential equations. Chem Eng Sci 2005;60:2609−19.
[24] Ergun S. Fluid flow through packed columns. Chem Eng Prog 1952;48:89−94.
[25] Hamers HP, Gallucci F, Williams G, van Sint Annaland M. Experimental demonstration of CLC and the pressure effect in packed bed reactors using $NiO/CaAl_2O_4$ as oxygen carrier. Submitted to Fuel 2014.
[26] Daubert TE, Danner RP. Data compilation tables of properties of pure compounds. New York: American Institute of Chemical Engineers; 1985.
[27] Barin I. Thermochemical data of pure substances. Weinheim: VCH; 1993.
[28] García-Labiano F, Adánez J, de Diego LF, Gayán P, Abad A, Cuadrat A. Effect of pressure on the behavior of copper-, iron-, and nickel-based oxygen carriers for chemical-looping combustion. Energy Fuels 2005;24:1402−13.
[29] Zafar Q, Abad A, Mattisson T, Gevert B, Strand M. Reduction and oxidation kinetics of $Mn_3O_4/Mg−ZrO_2$ oxygen carrier particles for chemical-looping combustion. Chem Eng Sci 2007;62:6556−67.
[30] Noorman S, Gallucci F, Van Sint Annaland M, Kuipers JAM. A theoretical investigation of CLC in packed beds. Part 1: particle model. Chem Eng J 2011;167:297−307.
[31] Dixon Anthony G, Cresswell David L. Theoretical prediction of effective heat transfer parameters in packed beds. AIChE J July 1979;25(4):663−76.
[32] Bauer R, Schluender EU. Effective radial thermal conductivity of packings in gas flow − 2. Thermal conductivity of the packing fraction without gas flow. Int Chem Eng 1978;18:189−204.
[33] Gunn DJ, Misbah MMA. Bayesian estimation of heat transport parameters in fixed beds. Int J Heat Mass Transf 1993;36:2209−21.
[34] Gunn DJ. Transfer of heat or mass to particles in fixed and fluidised beds. Int J Heat Mass Transf 1978;21:467−76.
[35] Edwards MF, Richardson JF. Gas dispersion in packed beds. Chem Eng Sci 1968;23:109−23.
[36] Hagen KD. Heat transfer with Applications. Upper Addle River, New Yersey, USA: Prentice Hall; 1999.
[37] Sinnott RK. Chemical engineering design, section 13.5. Chem. Eng. Des. Fourth. Oxford: Elsevier; 2005. p. 815.
[38] World steel prices. 2014. http://www.worldsteelprices.com.
[39] ThermalCeramics. JM23 saving you energy brochure. 2013. http://www.morganthermalceramics.com/products/insulating-Fire-Bricks-Ifb/.
[40] Seider WD, Seader JD, Lewin DR. Cost accounting and capital cost estimation (chapter 16). Prod. Process Des. Princ. Second. New York: John Wiley & Sons Inc; 2004. p. 473−562.
[41] Campanari S, Chiesa P, Manzolini G. CO_2 capture from combined cycles integrated with molten carbonate fuel cells. Int J Greenh Gas Control 2010;4: 441−51. http://dx.doi.org/10.1016/j.ijggc.2009.11.007.